https://doi.org/10.5194/egusphere-2024-405
Preprint. Discussion started: 15 March 2024

Emissions of Methane from Coal, Thermal power plants and Wetlands and its implications on Atmospheric Methane across the South Asian Region

Mahalakshmi D.Venkata[1]., Mahesh Pathakoti[1]*, A.Lakshmi Kanchana[1], Sujatha Peethani[2], Ibrahim Shaik[1], Krishnan Sundara Rajan[3], Vijay Kumar Sagar[4], Pushapanathan Raja[5], Yogesh K.Tiwari[4], Prakash Chauhan[1]

[1]National Remote Sensing Centre (NRSC), Indian Space Research Organisation (ISRO), Hyderabad, India-500037
[2]Formerly at The International Center for Agricultural Research in the Dry Areas
[3]Lab for Spatial Informatics, International Institute of Information Technology (IIIT), Hyderabad-5000084, India
[4]Indian Institute of Tropical Meteorology (IITM), Pune, India-411008.
[5]ICAR-Indian Institute of Soil and Water Conservation, Research Centre, Koraput, Odisha, India-763 002.

*Corresponding author: mahi952@gmail.com

Abstract

Atmospheric methane (CH_4) is a potent climate change agent responsible for a fraction of global warming. The present study investigated the spatial and temporal variability of atmospheric column-averaged (*X*) CH_4 (XCH_4) concentrations using Greenhouse gases Observing SATellite (GOSAT) and TROPOspheric Monitoring Instrument onboard the Sentienl-5 Precursor (S5P/TROPOMI) data from 2009 to 2022 over the South Asia region. During the study period, the long-term trends in XCH_4 increased from 1700 ppb to 1950 ppb with an annual growth rate of 8.76 ppb year^{-1}. Among all natural and anthropogenic sources of CH_4, the rate of increase in XCH_4 was higher over the Mundra thermal power station and Mundra ultra mega power plant at about 9.62 ppb year^{-1}, followed by the coal site at about 8.76 ppb year^{-1} (Korba). With a growth rate of 8.61 ppb year^{-1}, the Sundarbans natural wetland competes with coal sites, producing over 30 MT, indicating an equivalent anthropogenic source. For the 15 Indian Agroclimatic zones, significant high emissions of CH_4 were observed over the Middle Gangetic Plains (MGP), Trans Gangetic Plains (TGP), Upper Gangetic Plains (UGP), East Coast Plains & Hills (ECPH), Lower Gangetic Plains (LGP) and East Gangetic Plains (EGP). Further, the bottom-up anthropogenic CH_4 emissions data are mapped against the XCH_4 concentrations and found high correlation in the Indo Gangetic Plains (IGP) region, indicating the hotspots of anthropogenic CH_4. The present study highlighted the impact of natural and anthropogenic sources of XCH_4 and quantified the spatio-temporal changes in XCH_4 at each study site over the Indian region.

Keywords: GOSAT, S5P/TROPOMI, Column-averaged CH_4, South Asia, spatio-temporal, anthropogenic emissions.

https://doi.org/10.5194/egusphere-2024-405
Preprint. Discussion started: 15 March 2024

1. Introduction

Atmospheric methane (CH_4) is one of the high-potential greenhouse gases (GHG) that regulates the chemical reactions in the free troposphere and stratosphere. CH_4 has enormous potential for global warming, about 28–36 times that of CO_2 over 100 years (IPCC, 2021), and a comparatively short perturbation lifespan of about 12 years (Balcombe et al., 2018). Over the past decade, the research community has become more interested in anthropogenic CH_4 concentration due to its persistent rise in the atmosphere and lack of knowledge regarding its source or sink (Huang et al., 2015). The long-term observations from the National Oceanic and Atmospheric Administration (NOAA) have shown a yearly increase of 8 ppb CH4 $year^{-1}$, while Shadnagar an Indian site shows an increase of 10 ppb $year^{-1}$ (Sreenivas et al., 2022). Though the emissions have increased over the past 20 years, the causes are still not clearly understood. Recent research suggests that a combination of fossil fuel and agricultural emissions, with fluctuations in the CH_4 sink in the atmosphere, also plays a part (Schaefer et al., 2016; Worden et al., 2017; Turner et al., 2019; Zhang et al., 2022). The decadal budget indicates that relative uncertainties may range from 20 to 35 percent for inventories of anthropogenic emissions in specific sectors (food waste, agriculture, and fossil fuels), 50 to 100 percent for emissions from burning biomass and emissions from natural wetland ecosystems, and 100% or more for emissions from other natural sources. Geographically speaking, India's wetlands make up 4.7% of the nation's total land area (Bassi et al., 2014). The primary sources of CH_4 emissions include natural emissions from freshwater systems, wetlands, and geological sources; anthropogenic emissions come from waste management, agriculture, and the mining and burning of fossil fuels (Kirschke et al., 2013; Saunois et al., 2016a; Ganesan et al., 2019).

Wetlands are the natural sources that contribute to 20–40% of global emissions and dominate the inter-annual variability (Parker et al., 2018). Only limited studies have been carried out in India about discharge of methane from wetlands. A recent study (Vinna et al., 2021) shows that natural wetlands could produce 50% to 80% more CH_4 emissions by 2100. According to Schlesinger et al. (2009), wetlands, rice paddies, and ruminants are the leading producers of CH_4 on the Indian subcontinent. According to Hayashida et al. (2013), there is a seasonal pattern in the CH_4 concentration over monsoon Asia, with higher values during the post-monsoon and minimum in pre-monsoon. Along with temperature, precipitation, and radiation, the CH_4 emissions from the natural wetlands might affect the region's heat budgeting, exacerbating global warming on a local, regional, and even on global scale (Sakalli et al., 2017). Thermal power plants are responsible for a large amount of the GHG emissions from the energy sector. Each thermal power plant has a different set of emission factors for methane and nitrous oxide, which are based on operating conditions and combustion technology (Kang et al., 2019). The integrated measure of CH_4 includes contributions from the various vertical atmospheric layers, ranging from the Earth's surface measurement point to the uppermost layer of the atmosphere. Chandra et al. (2017) studied the raised air mass into the 600–200 hPa height layer over northern India accounts for 40% of the seasonal CH_4 augmentation during southwest monsoon season. Conversely, in the semi-arid

https://doi.org/10.5194/egusphere-2024-405
Preprint. Discussion started: 15 March 2024

region, the height over 600 hPa contributed up to approximately 88% of the amplitude of the XCH$_4$ seasonal cycle, while the atmosphere below 600 hPa contributed only around 12%. The feature of air mass transport processes in the Asian monsoon region is the main reason for the increased contributions from above 600 hPa across the northern Indian region.

Insufficient datasets exist about the CH$_4$ feedback originating from wetlands; a study on the precise estimation of CH$_4$ outflow from wetlands and its impact in local/regional global warming scenarios is therefore urgently needed. The ability to identify spatial and temporal fluctuations in atmospheric CH$_4$ from space, due to recent technological developments in remote sensing, could help fill in the gaps left by measurements performed by ships, planes, and the ground (Frankenberg et al., 2008; Kuze et al., 2009). The present study focuses on the Implications of emissions from Coal, Thermal power plants, and Wetlands on atmospheric methane over southsia using XCH$_4$ data from Greenhouse gases Observing SATellite (GOSAT) and TROPOspheric Monitoring Instrument onboard the Sentienl-5 Precursor (S5P/TROPOMI) from 2009 to 2022. It has further analyzed the spatial and temporal pattern of atmospheric CH$_4$ variations and emissions and its correlation with anthropogenic CH$_4$ emissions from the bottom-up emission inventory of EDGAR. The response of atmospheric CH$_4$ concentrations to anthropogenic emissions in various agroclimatic zones of India was further highlighted by this study using the XCH$_4$ data from 2001 to 2022.

2. Study region

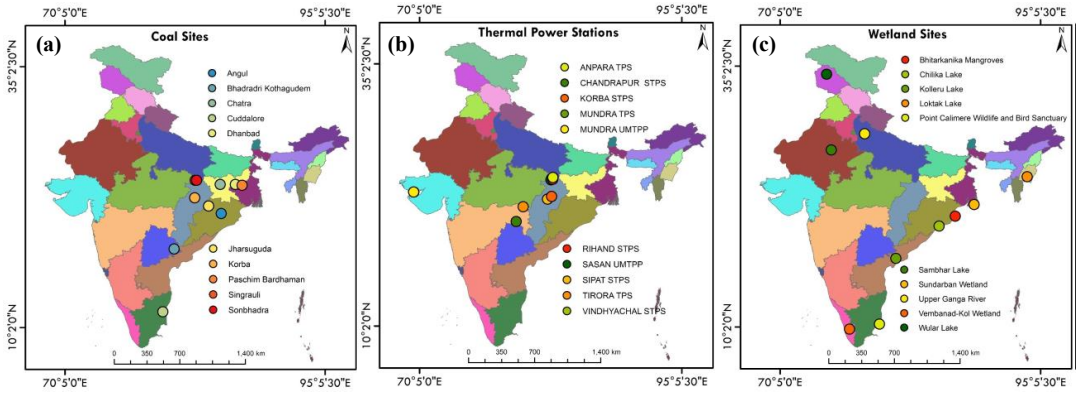

Figure 1 (a) The top 10 coal mine locations in India based on production (b) The locations of the top 10 thermal power stations and c) top 10 wetlands based on the area.

The distribution of heterogeneous sources of CH$_4$ over the Indian region are shown in Figure 1. Three heterogenic CH$_4$ source regions—coal fields, thermal power plants and the Ramsar Wetlands were the focus of the present study. The number of coal mines in India varies from 1 to 65, and the top ten coal fields were selected for this study based on their production capacity. During 2019–2020, coal and lignite production was between 0.1 and 120.47 MT. The study's coal mine details are provided in Table 2. Similarly, Table 3 lists thermal power stations according to

https://doi.org/10.5194/egusphere-2024-405
Preprint. Discussion started: 15 March 2024

their respective power generation. The Ramsar Convention is an international agreement created in 1971 to protect wetlands and promote their sustainable use (https://rsis.ramsar.org). The Ministry of Environment, Forests and Climate Change (MoEF&CC), Government of India, has identified 75 Ramsar Wetland sites in India as of November 2022. These sites span a total area of 13,35,530 ha. Based on the high total geographical area coverage (Table 1), the top 10 places were determined for the current investigation. The size varies from 423000 ha (Sundarbans Wetland, West Bengal) to 18900 ha (Wular Lake, Jammu and Kashmir).

3. Data and Methodology

For continuous monitoring of CO_2 and CH_4 from space, the level 2 (L2) column CH_4 (XCH_4) data obtained from the Greenhouse gases Observing SATellite (GOSAT) series developed by the Japan Aerospace Exploration Agency (JAXA) (Kuze et al., 2009). Onboard the GOSAT, the Thermal and Near Infrared Sensor for Carbon Observation Fourier-Transform Spectrometer (TANSO-FTS) is used to detect the CO_2 and CH_4 absorption spectra in the shortwave IR (1.60µm &2.0µm) region (Kuze et al., 2009). In the present study, the atmospheric CH_4 was obtained from 2009 to 2020 within a 100 km radius of the coal mines. The data corresponding to the quality flag (=0) was considered for the study only.

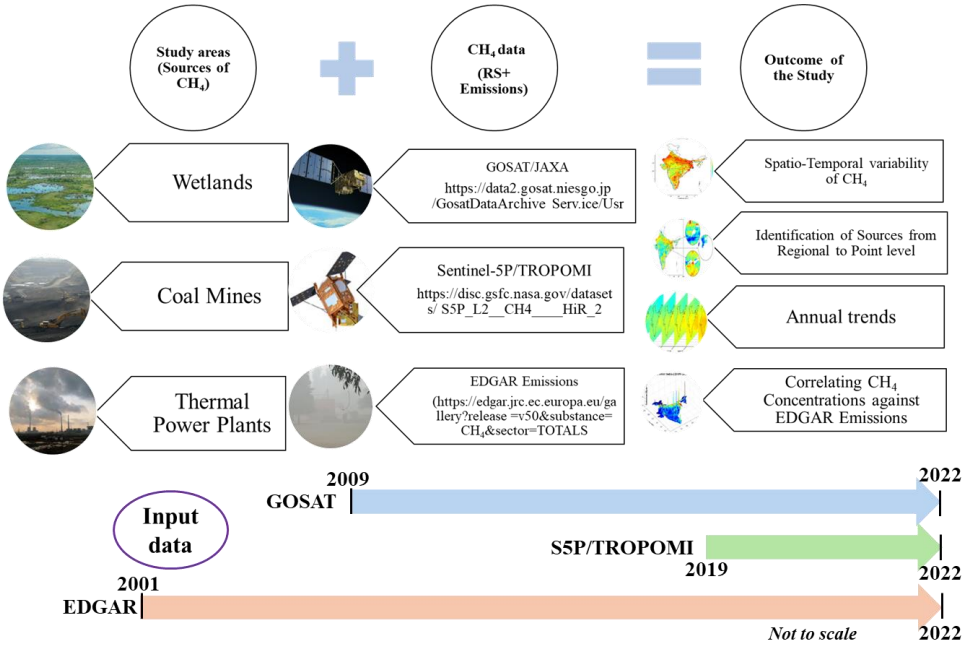

Figure 2 Data resources and Study approach

The Sentinel-5 Precursor satellite, which was launched on October 13, 2017, is equipped with the TROPOspheric Monitoring Instrument (TROPOMI), which tracks cloud characteristics, aerosols, and trace gases (Sentinel-5p. 2019). With a daily pass time of approximately 13:30 local solar time, the instrument's spectrometer measures reflected sunlight in the ultraviolet, visible, near-IR, and SWIR spectral windows. The CH_4 retrieval algorithm uses the two spectral bands, i.e.,

https://doi.org/10.5194/egusphere-2024-405
Preprint. Discussion started: 15 March 2024

reflectance in NIR (757-774nm) and SWIR (2305-2385nm) (Kozicka et al., 2023). Initially, retrievals based on TROPOMI had a high spatial resolution of 7 km x 3.5 km (along-track x across-track, Bergamaschi et al., 2022). From August 2019 to the present, the resolution has been increased to 5.5 km × 3.5 km (Sagar et al., 2022). The latest data version is now v2 from 2021-07-01 to now. The quality flag (<0.5) was only considered as per the product readme file document (Sentinel-5p. 2019). The data within the coal mines and wetlands area are taken from 01st May 2018 to 30th April, 2022. The individual shape files were given for each wetland field, and the satellite passes within the area were considered for the current study. As shown in Figure 2, a detailed procedure is explained in this section. The present study utilized the total anthropogenic emissions from the EDGAR (https://edgar.jrc.ec.europa.eu/gallery?release=v50&substance=CH4&sector=TOTALS, accessed on 01 November 2023) respectively.

We have selected the coal fields based on the production shown in Table 1. The data on all coal mines in India, their production, and their location are accessed from the https://dataverse.harvard.edu/dataset.xhtml?persistentId=doi:10.7910/DVN/TDEK8O. Each district has open cast or underground types of mines found in India, and the number of coal mines varies from 1 to 65. The coal/Lignite production was 0.1 to 120.47 MT during 2019-2020. The details of the coal mines in the present study are summarized in Table 1, and locations are mapped in Figure 1.

S.No	District names	No. of Mines	Production (MT)	Latitude	Longitude
1	Korba	15	120.47	22.47	82.56
2	Singrauli	7	82.19	24.15	82.6
3	Angul	13	80.61	20.97	85.11
4	Sonbhadra	5	47.36	24.15	82.74
5	Jharsuguda	9	36.71	21.69	83.89
6	Dhanbad	51	31.25	23.76	86.46
7	Paschim Bardhaman	65	31.23	23.68	87.11
8	Bhadradri Kothagudem	14	30.16	17.57	80.58
9	Chatra	4	29.65	23.76	85.01
10	Cuddalore	3	23.46	11.55	79.5

Table 1. The district names, the total number of coal mines, total production, and their centroid (latitudes and longitudes) locations of mines in the respective districts in 2019-2020.

The list is prepared based on the descending order of total production in each district in India. There are 262 thermal power stations with a full capacity of 229.335 GW and a total unit of 2689 in India, based on diesel, gas turbine, and steam as on March 31, 2020. Table 2 shows the list of thermal power stations.

https://doi.org/10.5194/egusphere-2024-405
Preprint. Discussion started: 15 March 2024

There are 11 Ramsar sites identified in 2022 (total 75 sites) by the Ministry of Environment Forest and Climate Change (MoEF&CC), India, covering a total area of 1,093,636 ha 2022. The present study considered the top 10 sites based on the high area coverage (Table 3) for the current study. The area ranges from 18900 ha (Wular Lake) to 423000 ha (Sundarban Wetland).

S.No	Power Stations names	Installed Capacity (MW)	No. of Units	Latitude (N)	Longitude (E)
1	Vindhyachal STPS	4760	13	24.1	82.68
2	Mundra TPS	4620	9	22.82	69.55
3	Mundra UMTPP	4000	5	22.82	69.53
4	Sasan UMTPP	3960	6	23.98	82.62
5	Tirora TPS	3300	5	21.41	79.97
6	Rihand STPS	3000	6	24.03	82.79
7	Sipat STPS	2980	5	22.14	82.29
8	Chandrapur STPS	2920	7	20	79.3
9	Anpara TPS	2630	7	24.21	82.8
10	Korba STPS	2600	7	22.39	82.68

Table 2. Top 10 thermal power plants based on their capacity.

S.No	Wetlands Location	Latitude (N)	Longitude (E)	Area (ha)
1	Sundarban Wetland	21.77	88.71	423000
2	Vembanad-Kol Wetland	9.83	76.75	151250
3	Chilika Lake	19.7	85.35	116500
4	Kolleru Lake	16.61	81.2	90100
5	Bhitarkanika Mangroves	20.65	86.9	65000
6	Point Calimere Wildlife and Bird Sanctuary	10.31	79.63	38500
7	Loktak Lake	24.43	93.81	26600
8	Upper Ganga River	28.55	78.2	26590
9	Sambhar Lake	27	75	24000
10	Wular Lake	34.26	74.55	18900

Table 3. Top 10 Wetlands fields based on their area coverage.

https://doi.org/10.5194/egusphere-2024-405
Preprint. Discussion started: 15 March 2024

4. Results and Discussion

4.1. Spatio-temporal variability of Space-based Atmospheric CH_4

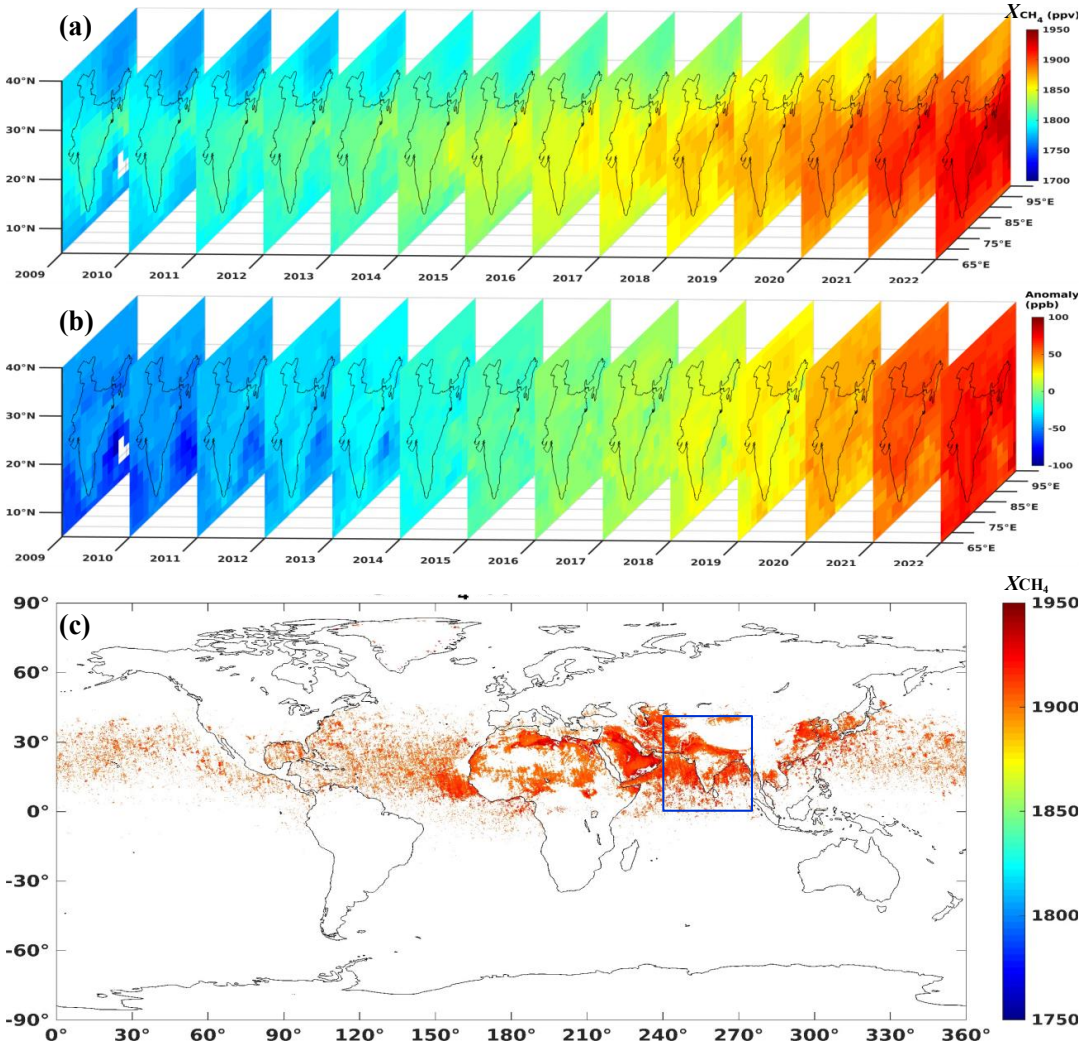

190 Figure 3 a) Remote Sensing (GOSAT) of atmospheric CH_4 variability over the Indian sub-continent b) anomaly during 2009 to 2022 and c) identification of probable high CH_4 concentration using S5P/TROPOMI data from 2019 to 2022.

In the present study, we examined the annual space-time distribution of the total column CH_4 (XCH_4) obtained from the GOSAT-1 and GOSAT-2 over South Asia as shown in Figures 3a-b
195 from 2009 to 2022 (N=14 years)—the long-term trends in XCH_4 increase from 1700 ppb to 1950 ppb from 2009 to 2022 with an annual growth rate of 8.76 ppb $year^{-1}$. This growth rate is statistically tested with a p-value less than 0.05 for n=3803 observations. A distinct, evident annual

https://doi.org/10.5194/egusphere-2024-405
Preprint. Discussion started: 15 March 2024

growth in CH_4 is seen over the Indian subcontinent. Figure 3b shows the spatio-temporal residuals calculated using the data from 2009 to 2022. Residuals indicate that the acceleration of CH_4 emissions in India has been significant since 2015. Before 2015, the CH_4 concentrations were nearly uniformly distributed. To identify the critical potential high emission zones of CH_4, the present study applied the 90th percentile statistical filter, as shown in Figure 3c. The percentile is often used to detect the points significantly different from the rest of the data. Statistically significant high concentrations of CH_4 are observed in tropical regions.

In the blue highlighted box, higher concentrations of CH_4 were observed in the Indo-Gangetic Plain (IGP) and northwest (NW) areas of India, southeast of China, and NW of China. Southern China and north China are marked with wetlands and rice paddy fields, which are the primary sources of CH_4. High concentrations of CH_4 over the IGP and NW are due to the population density and various industries that contribute to the emissions of CH_4 and emissions from the rice paddy fields, respectively. In the present study, Figure 1 also shows the locations of coal and thermal power plants in India. Globally, the tropical wetlands ecosystem accounts for about 20% of the total global source (Saunois et al., 2020; Shaw et al., 2022), evidenced by bottom-up and top-down inventories. The study in the following sections assessed the CH_4 growth rate associated with the source type over the Indian region.

Figure 4 shows the spatiotemporal distribution of XCH_4 as a function of latitude, which depicts the annual variability at each latitude covering the northern and southern hemispheres (SH). There is a transparent latitudinal gradient in space. A strong diffusion of CH_4 is observed from the northern hemisphere to SH during 2009 to 2022. During 2010, the XCH_4 was distributed nearly constantly at all latitudes, indicating the stability of emissions from natural and anthropogenic sources. However, the gradient between the NH and SH has narrowed down with a growth rate of 12 ppb year^{-1} in 2022, reflecting the dominance of anthropogenic emissions over the tropics and unidentified leaks from the tropical wetlands and natural gas (Rocher-Ros et al., 2023).

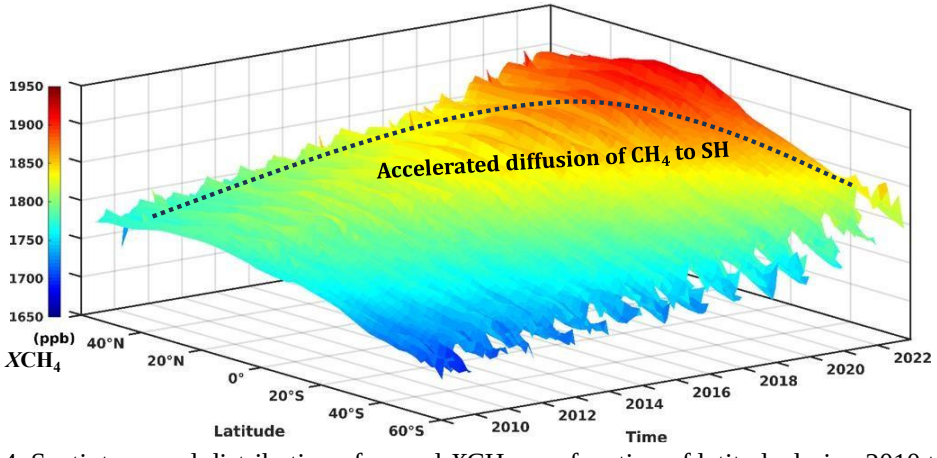

Figure 4. Spatiotemporal distribution of annual XCH_4 as a function of latitude during 2010 to 2022.

https://doi.org/10.5194/egusphere-2024-405
Preprint. Discussion started: 15 March 2024

More thoroughly, the characteristics of regional and global spatiotemporal variations are revealed by the continuous XCH_4 data in space and time. As shown in Figure 4, the XCH_4 displays a latitudinal gradient, and each latitudinal zone's growth tendencies are comparable.

4.2. Assessment of XCH_4 over different source types in India

Figures 5a-c shows the monthly time series of XCH_4 over the specific sources of CH_4 dotted in the Indian region during 2009 to 2020. Over the Indian sub-continent and south-east Asia, during October to November exhibits highest amounts of CH_4, while March through June often sees the lowest (Sreenivas et al., 2016; Song et al., 2023), because of the enormous diversity in the climate zones of the Asian region. The seasonal cycle (peak and trough) of XCH_4 is strongly associated with the vegetation during the active phase of cultivation and reduced photochemical reaction by the hydroxyl radicals, respectively.

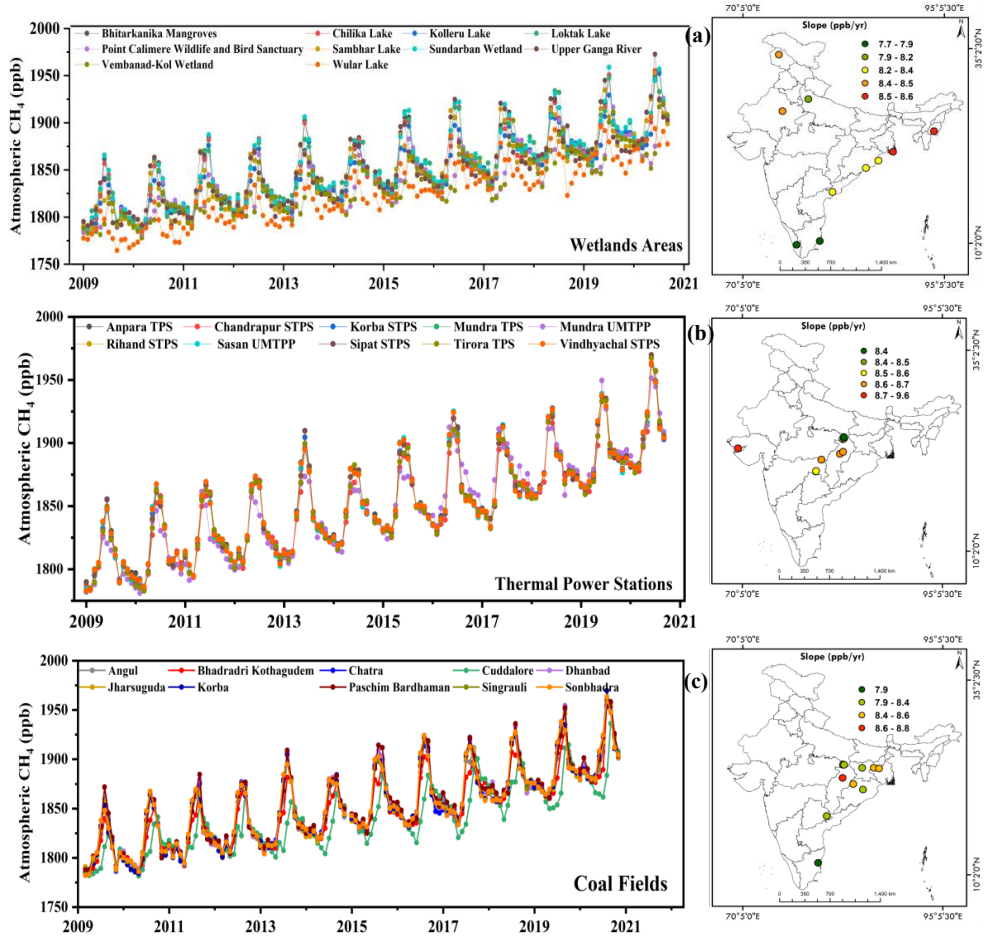

Figure 5. Monthly time series of XCH_4 over the a) Wetlands, b) Thermal power stations, and c) Coal fields: sources of emissions, along with the overall growth rate at the respective site.

https://doi.org/10.5194/egusphere-2024-405
Preprint. Discussion started: 15 March 2024

Over the coal, thermal, and wetlands, the XCH_4 shows typical seasonal behavior, with maximum activity during the post-monsoon (October-November) and minimum activity in the pre-monsoon (March-May), as shown in Figure 6. A seasonal maximum of XCH_4 was observed over Coal and Thermal power plants from September to October and a minimum in pre-monsoon (March-May). In the case of wetlands, a shift in seasonal maxima varies from site to site, indicating their respective active phase of methanogens and the magnitude of the seasonal amplitude, which runs as a function of the individual wetland area. A natural process known as methanogenesis causes wetlands to create CH_4. Methanogens are microscopic organisms that break down organic substances in an oxygen-free environment. Thus, wetlands are perfect for methanogens to grow and release CH_4 since they are usually oxygen-poor, moist habitats (Zhang et al., 2023). Therefore, the present study investigated the above-listed wetlands; Sundarbans wetland (Area = 423000 ha) exhibits a high concentration of CH_4 with pronounced seasonality and lower concentrations over Wular Lake (area = 18900 ha).

During the examination period, the seasonal trends (slope) at each location, as summarised in Tables 1-3, were evaluated using Sen's slope-based Mann-Kendall test with a significance of p-value < 0.05 (Pathakoti et al., 2021). The rate of increase in XCH_4 was higher over the Sundarbans wetland, West Bengal, with a slope of 8.61 ppb $year^{-1}$ and followed by the Loktak Lake (area=26600 ha), northeastern region (slope =8.60 ppb $year^{-1}$). The Vembanad-Kol wetland in Kerala is the country's second most extensive wetlands (area = 151250 ha). However, the rate of increase of XCH_4 is slower (slope =7.73 ppb $year^{-1}$) among the top 10 wetlands. This study indicates that the Sundarbans and Loktak Lakes are rich in moist habitats that act as positive feedback to the leaks of CH_4 into the atmosphere. An exciting phenomenon between the Loktak Lake and the Vembanad-Kol wetland was observed with an unexpectedly low growth rate of XCH_4 over the Vembanad-Kol wetland. This phenomenon indicates that compared to other wetlands in India, the Vembanad-Kol wetland could reduce CH_4 emissions through the methanotrophic process. Typically, the Indian climate is hot and humid, causing disturbances in the rainfall patterns; an increase in the waterlogged soils expands the wetlands (Zhang et al., 2023). Typical tropical wetlands are acting as positive feedback to climate change (Salimi et al., 2021).

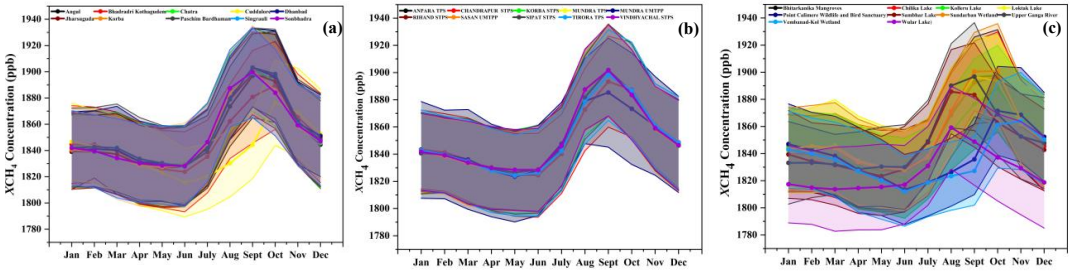

Figure 6. Seasonal XCH_4 over a) Coal fields, b) Thermal power stations and c) Wetlands.

https://doi.org/10.5194/egusphere-2024-405
Preprint. Discussion started: 15 March 2024

Irrespective of the power production capacity, over the thermal power plants, the CH_4 exhibited stabilized seasonality at each location. However, the growth rate of XCH_4 was higher over the Mundra thermal power station (TPS) and Mundra ultra mega power plant (UMPP), Gujarat, with a slope of about 9.62 ppb year^{-1}, from 2009 to 2020. The Mundra TPS and UMPP, Gujarat, have a total power capacity of 8620 MW with 14 units. With 2630 MW installed power capacity, the Anapara TPS exhibited an XCH_4 growth rate of 8.40 ppb year^{-1}. This indicates that the higher potential power plants contribute more CH_4 emissions into the atmosphere. Over the coal mines, The Korba (120.47 Mega tons-MT, 120 mines) shows high XCH_4 trend about 8.76 ppb year^{-1}, Jharsuguda (36.71 MT, 9 mines), Dhanbad (31.25 MT, 51 mines), and Paschim Bardhaman (31.23 MT, 65 mines) show an increase of XCH_4 with an annual trend of 8.64 ppb year^{-1}. The lowest annual trend in XCH_4 was observed over the Cuddalore coal mine (23.46 MT, 3 mines), which was about 7.92 ppb year^{-1}. Figure 8 shows the continuous XCH_4 data from the S5P/TROPOMI at 0.05º×0.05º, complementing the GOSAT efforts in monitoring the XCH_4 dynamics in space and time. We demonstrated the spatiotemporal variation characteristics of XCH_4 more comprehensively at three different source type locations (Wetland, coal, and thermal power plant). High XCH_4 concentrations over the coal and thermal power station sites and relatively lower concentrations in the wetland site. We concluded that the high-resolution S5P/TROPOMI has the potential to detect the point source variability. The growth rate of XCH_4 over the Sundarbans (India's most significant) natural wetland competes with coal sites with the production of over 30 MT, indicating an equivalent anthropogenic source. Results of the analysis in the context of thermal power plants and coal mines indicate that the emissions from the fossil fuels industries are significant, and the release of CH_4 into the atmosphere is commensurate with the production of the power and mining capacity.

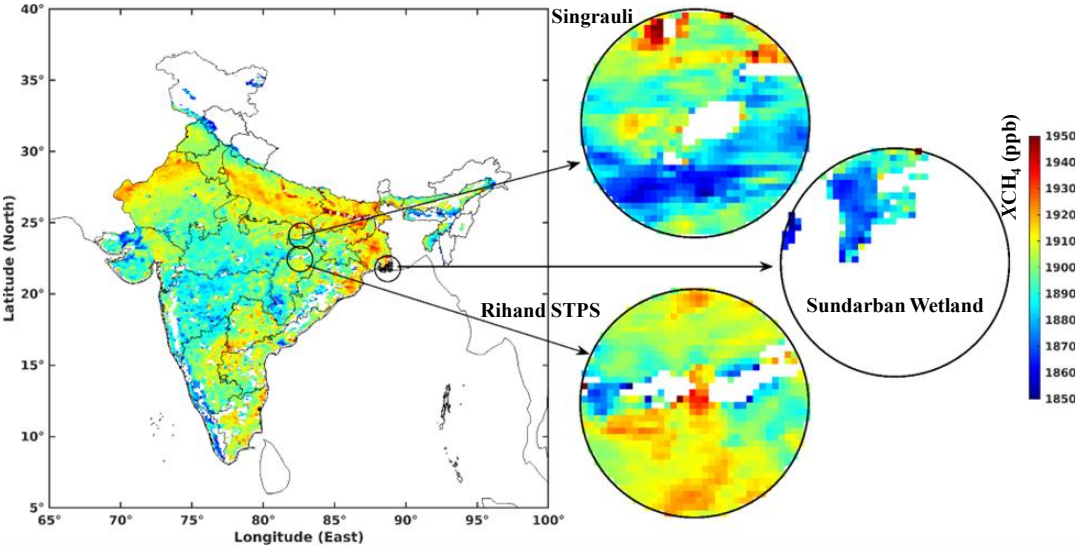

Figure 7. S5P/TROPOMI XCH_4 gridded to 0.05° × 0.05° over Indi and XCH_4 over wetland, coal, and thermal power plant sites with a radius of 100 km.

https://doi.org/10.5194/egusphere-2024-405
Preprint. Discussion started: 15 March 2024

4.3. CH_4 emissions over India's Agroclimatic zones

India is divided into 15 agroclimatic zones according to the combination of soil types and climatic conditions. These zones offer a structure for the nation's development and execution of agricultural policies and practices. The crops and farming methods that are most appropriate for the environmental conditions in each zone are distinct from one another. Out of natural and anthropogenic sources of CH_4, agricultural activity is also one of the dominant contributors to CH_4 dynamics in the atmosphere. Figures 8a-c show India's 15 agroclimatic zones and spatiotemporal trends of CH_4 emissions obtained from the bottom-up emission inventory of EDGAR (Crippa et al., 2020) from 2001 to 2022. Significant high emissions of CH_4, as shown in Figure 7c, were observed over the Middle Gangetic Plains-MGP (2), Trans Gangetic Plains-TGP (3), Upper Gangetic Plains-UGP (4), East Coast Plains & Hills-ECPH (7), Lower Gangetic Plains-LGP (14) and East Gangetic Plains-EGP (15). These agroclimatic zones have active farming in rice, wheat, sugarcane, maize, millet, gram, cotton, etc. Besides traditional farming, the Lower Gangetic Plains has also actively contributed to livestock, horticulture, and forage production (Ahmad et al., 2017). Among all 15 agroclimatic zones, the MGP, TGP, UGP, ECPH, LGP and EGP have exhibited high emissions of CH4 indicating the diversification of agricultural practices and homogenous traditions of agricultural production. Rice- wheat (R-W) based production system are mainly being practiced in this region which is causing the negative effects on climate. (Taneja et al., 2019). CH_4 emissions over the Northwest region is exhibiting weak contribution compared to other agroclimatic zones of India.

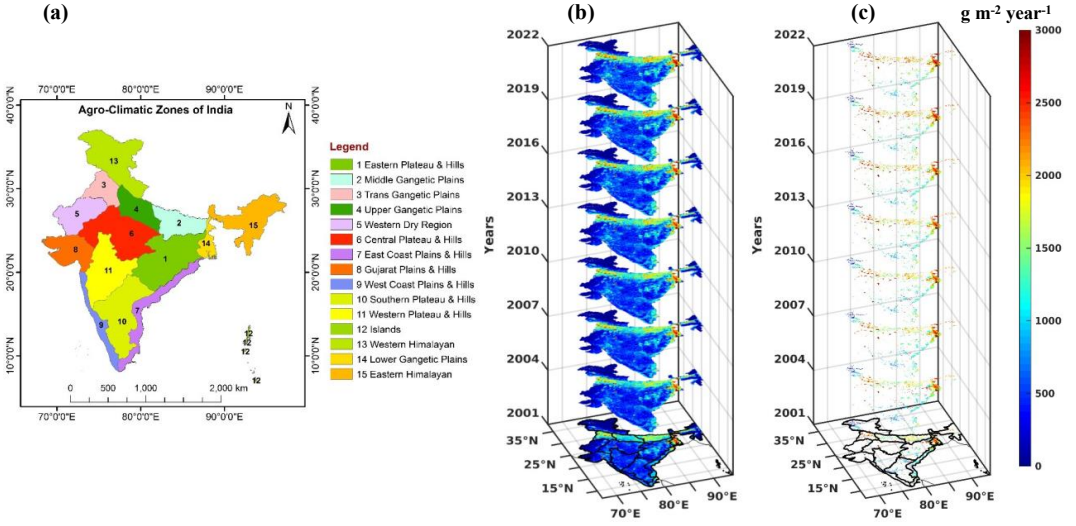

Figure 8. a) Agroclimatic zones of India, b) bottom-up CH_4 emissions inventory of EDGAR and c) 90th percentile statistical filter applied CH_4 emissions from 2001 to 2022.

https://doi.org/10.5194/egusphere-2024-405
Preprint. Discussion started: 15 March 2024

4.4. Spatial correlation between XCH_4 Concentrations and Emissions over India

To understand the relationship between India's high XCH_4 concentration zones against emissions, we have computed pixel-level correlation between S5P/TROPOMI measured XCH_4 concentrations and bottom-up inventory of EDGAR-based XCH_4 anthropogenic emissions. Figures 9a-c show XCH_4 concentrations from S5P/TROPOMI, EDGAR-based anthropogenic emissions, and their correlation coefficient. The spatial patterns of XCH_4 concentrations agree well with the high-emission regions. The correlation coefficient 'r' is strongly positive on in the IGP region, shows that more CH_4 emission into the atmosphere through rapid industrial activity and anthropogenic contribution from human activity due to high population density. Besides the IGP region, the 'r' value is also strong in the east and northeast region due to the active anthropogenic emissions from natural sources such as agricultural activities, livestock, and wetlands (Behera et al., 2022).

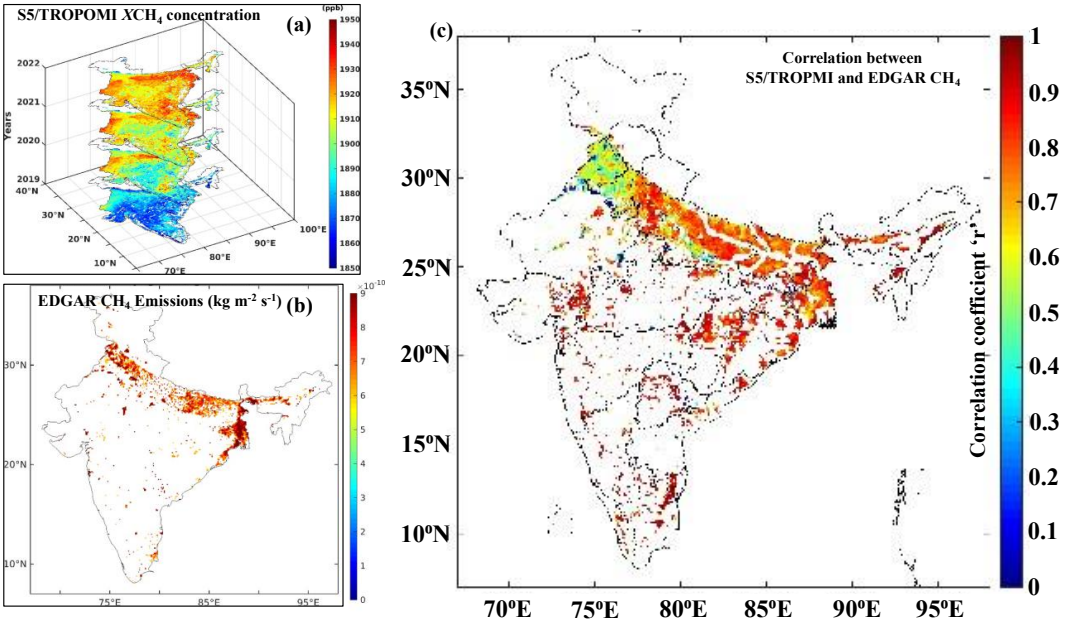

Figure 9. Pixel level correlation between S5/TROPOMI based XCH_4 and anthropogenic CH_4 bottom-up emission inventory of EDGAR during 2019 to 2022.

5. Conclusion

Since the beginning of the Industrial Revolution, growing human populations have resulted in increased waste production, agriculture, and the use of fossil fuels. Therefore, this study demonstrated the spatiotemporal dynamics of XCH_4 in the atmosphere and associated natural (wetlands) and anthropogenic sources (coal fields and thermal power plants) in the Indian region. The present study utilised the remote sensing based XCH_4 data from the GOSAT and S5P/TROPOMI from 2009 to 2022. The following are the salient findings of the study.

https://doi.org/10.5194/egusphere-2024-405
Preprint. Discussion started: 15 March 2024

- The present study demonstrated the continuous XCH$_4$ data from the S5P/TROPOMI and GOSAT to effectively monitor the XCH$_4$ dynamics in space and time.
- Long-term temporal and spatial distribution characteristics and variations of CH$_4$ emissions in India have accelerated in the last decade and globally, a substantial diffusion of CH$_4$ is observed from the northern to southern hemisphere.
- Long-term trends of XCH$_4$ show significant annual growth from 2009 to 2022 in CH$_4$ over the Indian subcontinent, with a yearly growth rate of 8.76 ppb which is in line with the global trend.
- XCH$_4$ levels peak in September-October over Coal and Thermal power plants but reach their minimum during March-May. The seasonal maxima of wetlands vary from site to site and are related to their size and active phase of methanogens.
- , The reduced CH$_4$ concentration in the Vembanad-Kol wetland of India as compared to other wetlands indicates the active methanotrophic process, as evidenced by the slow growth rate of XCH$_4$.
- A high XCH$_4$ trend of ≈ 8.76ppb year^{-1} with a high slope of about 9.62 ppb year^{-1} from the Mundra TPS and Mundra UMPP in Gujarat, as well as the Korba coal mine indictaing elevated and significant emissions from the fossil fuels industries as compared to other natural sources.
- The high levels of CH$_4$ emissions seen in the MGP, TGP, UGP, ECPH, LGP, and EGP agroclimatic zones may be related to the varied farming methods and traditional agricultural output in these regions. Most of these areas revolve around the Rice- Wheat farming system which is negatively impacting the climate.
- The spatial patterns of XCH$_4$ concentrations agree well with the high-emission regions. The correlation coefficient 'r' is strongly agreed in the IGP region.

Therefore we conclude that the space based XCH$_4$ dataset provides significant support to track long term changes in CH$_4$ and provides insightful information on the causes and feedback mechanisms for the elevated concentrations of methane across the south Asia region.

Code and data availability

The GOSAT, TROPOMI satellite data and EDGAR bottom up inventory data used in the present study are freely available and can be downloaded as summarised in Figure 2 with the user's credentials. The code will be available from the author upon request.

Declaration of Interest Statement

Authors declare no conflict of interest.

https://doi.org/10.5194/egusphere-2024-405
Preprint. Discussion started: 15 March 2024

Author Contribution

D.V. Mahalakshmi: Formal analysis, Writing – original draft. Mahesh P: Conceptualization, Formal analysis, Writing – original draft. A.L.Kanchana: Formal analysis, Writing – original draft. Sujatha. P: Formal data analysis, Writing – original draft. Ibrahim Shaik: Analysis. K.S. Rajan: Writing-review and Editing. Vijay Kumar Sagar: Formal Analysis and data curation. P. Raja: Writing-review and Editing. Y.K.Tiwari: Writing reviewing and Editing. Prakash Chauhan: Writing-review and Editing.

Acknowledgement

We sincerely thank the Director, NRSC/ISRO, for his kind guidance and support. Authors greatly acknowledge the JAXA and National Institute of Environmental Studies (NIES) for providing free access to the GOSAT *X*CH_4 observations (https://data2.gosat.niesgo.jp /GosatDataArchive Serv.ice/usr/ download accessed on 15 June 2023) and the Earthdata for giving access to the S5P/TROPOMI (https://disc.gsfc.nasa.gov/datasets/ S5P_L2__CH4____HiR_2/summary accessed on 15 June 2023) data. We also thank the European Commission's Joint Research Centre (JRC) for providing the CH4 bottom-up inventory of EDGAR (https://edgar.jrc.ec.europa.eu/gallery?release =v50&substance= CH4&sector=TOTALS, accessed on 25 July 2023. This work has been carried out as part of TDP titled "Investigation of Atmospheric GHGs Emissions over the Indian Region (AGE)" and the Land- Ocean-Atmospheric GHGs Interaction Experiments (LOAGIN-X) of Climate and Atmospheric Processes of IGBP programme.

References

1. Ahmad, L., Habib Kanth, R., Parvaze, S., Sheraz Mahdi, S., Ahmad, L., Habib Kanth, R., Parvaze, S. and Sheraz Mahdi, S., 2017. Agro-climatic and agro-ecological zones of India.
2. Balcombe, P., Speirs, J. F. , Brandon, N. P. , & Hawkes, A. D. (2018). Methane emissions: Choosing the right climate metric and time horizon. *Environmental Science: Processes and Impacts*, 20(10), 1323–1339. 10.1039/C8EM00414E.
3. Bassi, N., Dinesh, K.M., Anuradha, S., and PardhaSaradhi, P. (2014). Status of wetlands in India: A review of extent, ecosystem benefits, threats and management strategies. J. Hydrol. Reg. Stud 2, 1.
4. Behera, M.D., Mudi, S., Shome, P., Das, P.K., Kumar, S., Joshi, A., Rathore, A., Deep, A., Kumar, A., Sanwariya, C. and Kumar, N., 2022. COVID-19 slowdown induced improvement in air quality in India: Rapid assessment using Sentinel-5P TROPOMI data. Geocarto International, 37(25), pp.8127-8147.
5. Bergamaschi, P., Segers, A., Brunner, D., Haussaire, J.M., Henne, S., Ramonet, M., Arnold, T., Biermann, T., Chen, H., Conil, S. and Delmotte, M., 2022. High-resolution

https://doi.org/10.5194/egusphere-2024-405
Preprint. Discussion started: 15 March 2024

inverse modelling of European CH 4 emissions using the novel FLEXPART-COSMO TM5 4DVAR inverse modelling system. Atmospheric Chemistry and Physics, 22(20), pp.13243-13268.

6. Chandra, N., Hayashida, S., Saeki, T., & Patra, P. K. (2017). What controls the seasonal cycle of columnar methane observed by GOSAT over different regions in India?. *Atmospheric Chemistry and Physics*, *17*(20), 12633-12643.
7. Crippa, M., Solazzo, E., Huang, G., Guizzardi, D., Koffi, E., Muntean, M., Schieberle, C., Friedrich, R. and Janssens-Maenhout, G., 2020. High resolution temporal profiles in the Emissions Database for Global Atmospheric Research. Scientific data, 7(1), p.121.
8. Frankenberg, C., Aben, I. P. B. J. D. E., Bergamaschi, P., Dlugokencky, E. J., Van Hees, R., Houweling, S., ... & Tol, P. (2011). Global column-averaged methane mixing ratios from 2003 to 2009 as derived from SCIAMACHY: Trends and variability. *Journal of Geophysical Research: Atmospheres*, *116*(D4).
9. Ganesan, A. L., Schwietzke, S., Poulter, B., Arnold, T., Lan, X., Rigby, M., Vogel, F. R., van der Werf, G. R., Janssens-Maenhout, G., Boesch, H., Pandey, S., Manning, A. J., Jackson, R. B., Nisbet, E. G., and Manning, M. R.: Advancing scientific understanding of the global methane budget in support of the Paris Agreement, Global Biogeochem. Cy., 33, 1475–1512, https://doi.org/10.1029/2018GB006065, 2019.
10. Goroshi, S. K., Singh, R. P., Panigrahy, S., & Parihar, J. S. (2011). Analysis of seasonal variability of vegetation and methane concentration over India using SPOT-VEGETATION and ENVISAT-SCIAMACHY data. *Journal of the Indian Society of Remote Sensing*, *39*, 315-321.
11. Goroshi, S. K., Singh, R. P., Panigrahy, S., and Parihar, J. S.: Analysis of seasonal variability of vegetation and methane concentration over India using SPOT-VEGETATION and ENVISATSCIAMACHY data, J. Indian Soc. Remote Sens., 39, 315–321, 2011.
12. Hayashida, S., Ono, A., Yoshizaki, S., Frankenberg, C., Takeuchi, W., and Yan, X.: Methane concentrations over Monsoon Asia as observed by SCIAMACHY: signals of methane emission from rice cultivation, Remote Sens. Environ., 139, 246–256, https://doi.org/10.1016/j.rse.2013.08.008, 2013.
13. Huang, L., Tang, M., Fan, M., & Cheng, H. (2015). Density functional theory study on the reaction between hematite and methane during chemical looping process. *Applied Energy*, *159*, 132-144.
14. IPCC . (2021). *Climate change 2021: The physical science basis. Contribution of Working Group I to the sixth assessment report of the intergovernmental panel on climate change*.
15. Kang, M., Mauzerall, D. L., Ma, D. Z., & Celia, M. A. (2019). Reducing methane emissions from abandoned oil and gas wells: Strategies and costs. *Energy Policy*, *132*, 594-601.
16. Kirschke, S., Bousquet, P., Ciais, P., Saunois, M., Canadell, J. G., Dlugokencky, E. J., Bergamaschi, P., Bergmann, D., Blake, D. R., Bruhwiler, L., Cameron-Smith, P., Castaldi, S., Chevallier, F., Feng, L., Fraser, A., Heimann, M., Hodson, E. L., Houweling, S., Josse,

https://doi.org/10.5194/egusphere-2024-405
Preprint. Discussion started: 15 March 2024

B., Fraser, P. J., Krummel, P. B., Lamarque, J.- F., Langenfelds, R. L., Quéré, C. L., Naik, V., O'Doherty, S., Palmer, P. I., Pison, I., Plummer, D., Poulter, B., Prinn, R. G., Rigby, M., Ringeval, B., Santini, M., Schmidt, M., Shindell, D. T., Simpson, I. J., Spahni, R., Steele, L. P., Strode, S. A., Sudo, K., Szopa, S., Werf, G. R. van der, Voulgarakis, A., Weele, M. van, Weiss, R. F., Williams, J. E., and Zeng, G.: Three decades of global methane sources and sinks, Nat. Geosci., 6, 1–11, https://doi.org/10.1038/ngeo1955, 2013.

17. Kozicka, K., Orazalina, Z., Gozdowski, D., & Wójcik-Gront, E. (2023). Evaluation of temporal changes in methane content in the atmosphere for areas with a very high rice concentration based on Sentinel-5P data. *Remote Sensing Applications: Society and Environment*, *30*, 100972.

18. Kuze, A., Suto, H., Nakajima, M. and Hamazaki, T., 2009. Thermal and near infrared sensor for carbon observation Fourier-transform spectrometer on the Greenhouse Gases Observing Satellite for greenhouse gases monitoring. Applied optics, 48(35), pp.6716-6733.

19. Lan, X., K.W. Thoning, and E.J. Dlugokencky: Trends in globally-averaged CH4, N2O, and SF6 determined from NOAA Global Monitoring Laboratory measurements. Version 2024-01, https://doi.org/10.15138/P8XG-AA10

20. Parker, R. J., Boesch, H., McNorton, J., Comyn-Platt, E., Gloor, M., Wilson, C., ... & Bloom, A. A. (2018). Evaluating year-to-year anomalies in tropical wetland methane emissions using satellite CH4 observations. *Remote Sensing of Environment*, *211*, 261-275.

21. Parker, R.J., Boesch, H., McNorton, J., Comyn-Platt, E., Gloor, M., Wilson, C., Chipperfield, M.P., Hayman, G.D. and Bloom, A.A., 2018. Evaluating year-to-year anomalies in tropical wetland methane emissions using satellite CH4 observations. Remote Sensing of Environment, 211, pp.261-275.

22. Pathakoti, M., Santhoshi, T., Aarathi, M., Mahalakshmi, D.V., Kanchana, A.L., Srinivasulu, J., SS, R.S., Soni, V.K., MVR, S.S. and Raja, P., 2021. Assessment of spatio-temporal climatological trends of ozone over the Indian region using machine learning. Spatial Statistics, 43, p.100513.

23. Rocher-Ros, G., Stanley, E.H., Loken, L.C., Casson, N.J., Raymond, P.A., Liu, S., Amatulli, G. and Sponseller, R.A., 2023. Global methane emissions from rivers and streams. Nature, 621(7979), pp.530-535.

24. S. Pai and H. Zerriffi, "A novel dataset for analysing sub-national socioeconomic developments in the Indian coal industry," IOP SciNotes, vol. 2, no. 1, p. 014001, Mar. 2021, doi: 10.1088/2633-1357/abdbbb.

25. Sagar, V. K., Pathakoti, M., Mahalakshmi, D. V., Rajan, K. S., MVR, S. S., Hase, F., ... & Sha, M. K. (2022). Ground-Based Remote Sensing of Total Columnar CO 2, CH 4, and CO Using EM27/SUN FTIR Spectrometer at a Suburban Location (Shadnagar) in India and Validation of Sentinel-5P/TROPOMI. *IEEE Geoscience and Remote Sensing Letters*, *19*, 1-5.

https://doi.org/10.5194/egusphere-2024-405
Preprint. Discussion started: 15 March 2024

26. S. Salimi., S.A.A.A.N. Almuktar and M. Scholz (2021). Impact of climate change on wetland ecosystems: A critical review of experimental wetlands, Journal of Environmental Management, https://doi.org/10.1016/j.jenvman.2021.112160
27. Sakalli, A., Cescatti, A., Dosio, A., & Gücel, M. U. (2017). Impacts of 2 C global warming on primary production and soil carbon storage capacity at pan-European level. *Climate Services*, *7*, 64-77.).
28. Saunois M et al 2016a The global methane budget 2000-2012 Earth Syst. Sci. Data 8 697–751
29. Schaefer, H., Fletcher, S. E. M., Veidt, C., Lassey, K. R., Brailsford, G. W., Bromley, T. M., Dlugokencky, E. J., Michel, S. E., Miller, J. B., Levin, I., Lowe, D. C., Martin, R. J., Vaughn, B. H., and White, J. W. C.: A 21st century shift from fossil-fuel to biogenic methane emissions indicated by 13CH4, Science, 352, https://doi.org/10.1126/science.aad2705, 2016.
30. Schneising, O., Buchwitz, M., Burrows, J. P., Bovensmann, H., Bergamaschi, P., and Peters, W.: Three years of greenhouse gas column-averaged dry air mole fractions retrieved from satellite – Part 2: Methane, Atmos. Chem. Phys 9, 443–465, doi:10.5194/acp-9-443-2009, 2009.
31. Shaw, Jacob T., et al. "Large Methane Emission Fluxes Observed from Tropical Wetlands in Zambia." 2022, https://doi.org/10.1029/2021GB007261.
32. Song, H., Sheng, M., Lei, L., Guo, K., Zhang, S. and Ji, Z., 2023. Spatial and Temporal Variations of Atmospheric CH4 in Monsoon Asia Detected by Satellite Observations of GOSAT and TROPOMI. Remote Sensing, 15(13), p.3389.
33. Sreenivas, G., Mahesh, P., Subin, J., Kanchana, A. L., Rao, P. V. N., &Dadhwal, V. K. (2016). Influence of meteorology and interrelationship with greenhouse gases (CO2 and CH4) at a suburban site of India. Atmospheric Chemistry and Physics, 16, 3953-3967,doi.org/10.5194/acp-16-3953-2016.
34. Sreenivas, G., P. Mahesh, D. V. Mahalakshmi, A. L. Kanchana, Naveen Chandra, Prabir K. Patra, P. Raja, Shesha Sai MVR, Sripada S, Rao PV, Dadhwal VK. (2022). Seasonal and annual variations of CO_2 and CH_4 at Shadnagar, a semi-urban site. *Science of The Total Environment*, 819:153114, https://doi.org/10.1016 /j.scitotenv.2022.1 53114.
35. Taneja, G., Pal, B.D., Joshi, P.K., Aggarwal, P.K. and Tyagi, N.K., 2019. Farmers' preferences for climate-smart agriculture—an assessment in the Indo-Gangetic Plain (pp. 91-111). Springer Singapore.
36. Turner, A. J., Frankenberg, C., and Kort, E. A.: Interpreting contemporary trends in atmospheric methane, P. Natl. Acad. Sci. USA, 116, 2805–2813, https://doi.org/10.1073/pnas.1814297116, 2019
37. Vinna˚, L., Medhaug, I., and Schmid, M. (2021). The vulnerability of lakes to climate change along an altitudinal gradient. Commun. Earth Environ. 2, 35.
38. Worden, J. R., Bloom, A. A., Pandey, S., Jiang, Z., Worden, H. M., Walker, T. W., Houweling, S., and Röckmann, T.: Reduced biomass burning emissions reconcile

https://doi.org/10.5194/egusphere-2024-405
Preprint. Discussion started: 15 March 2024

conflicting estimates of the post-2006 atmospheric methane budget, Nat. Commun., 8, 1–11, https://doi.org/10.1038/s41467-017-02246-0, 2017.

39. Zhang, L., Tian, H., Shi, H., Pan, S., Chang, J., Dangal, S. R., ... & Jackson, R. B. (2022). A 130-year global inventory of methane emissions from livestock: Trends, patterns, and drivers. *Global Change Biology*, *28*(17), 5142-5158.
40. Zhang, Z., Poulter, B., Feldman, A.F., Ying, Q., Ciais, P., Peng, S. and Li, X., 2023. Recent intensification of wetland methane feedback. Nature Climate Change, 13(5), pp.430-433.